J. Fluid Mech. (2020), *vol.* 897, A13. © The Author(s), 2020.
Published by Cambridge University Press
doi:10.1017/jfm.2020.377

Tidal diffraction by a small island or cape, and tidal power from a coastal barrier

Chiang C. Mei†

Department of Civil and Environmental Engineering, Massachusetts Institute of Technology, Cambridge, MA 02139-4307, USA

(Received 12 January 2020; revised 3 April 2020; accepted 5 May 2020)

The tidal waves scattered by a small island and a small cape of elliptical shape are derived by the method of matched asymptotics. The results complement the irrotational flow approximation of the near field by Proudman (*Proc. Lond. Math. Soc.*, vol. 14, 1915, pp. 89–102). The potential for harnessing tidal power is assessed for the limiting case of a coast-connected thin dam.

Key words: waves in rotating fluids, wave–structure interactions, coastal engineering

1. Introduction

The theory of scattering of long waves by small bodies has a long history that can be traced back to Lord Rayleigh (Strutt 1897) in his treatment of aerial and electric waves. The formal procedure of matched asymptotics has been applied in many areas of wave propagation and extended to higher orders, subjected to either Dirichlet or Neumann boundary conditions. Extensive reviews can be found in the articles by Crighton & Leppington (1973), Martin & Dalrymple (1988), Kleinman & Vainberg (1994) and Guo & McIver (2011) and in the books by Varadan & Varadan (1968) and Martin (2006), mostly for sound waves in solids and fluids in a non-rotating system.

Affected by the Earth's rotation, tidal diffraction by large coastline features has been reviewed comprehensively by LeBlond & Mysak (1987). Other relevant works include Crease (1956) for a semi-infinite barrier, Buchwald (1971) for a cornered coast, Buchwald & Miles (1974) for a gap in a long barrier, Pinsent (1971) for a depth discontinuity, Pinsent (1972) for small irregularities along a straight coast, and Howe & Mysak (1973) for a randomly irregular coastline, etc. However, for tides around islands of finite size, analytical theories are relatively scarce. Proudman (1915) obtained the exact solution for a circular island and treated a small elliptical cape and its limit of a thin barrier protruding from a coast, but confined his analysis to the near field by employing the potential theory approximation. Refraction and diffraction of Rossby waves by a long step and a ridge near slowly varying one-dimensional bathymetry were first analysed by Rhines (1969*a*). Two-dimensional diffraction by islands and seamounts of circular geometries was also covered by Rhines (1969*b*).

† Email address for correspondence: ccmei@mit.edu

While tidal diffraction excluding the β effect is governed by the familiar Helmholtz equation, the oblique derivative boundary condition due to the Coriolis parameter f,

$$\frac{\partial \zeta}{\partial n} - \mathrm{i}\frac{f}{\omega}\frac{\partial \zeta}{\partial s} = 0, \tag{1.1}$$

is of neither Dirichlet nor Neumann form. Analytical theories for finite scatterers of general size and geometry are known to be difficult (Krutitskii 2001). Explicit numerical computations based on integral equations for an island in a sea of constant depth have been reported by Abel-Hafz, Essawy & Moubark (1997), who imposed the Neumann boundary condition on the coast instead of (1.1). Al-Hawaj, Essawy & Faltas (1991) computed tidal impact on coastal irregularities by ignoring the Earth's rotation in the approximate Green's function. Hence the effect of the Earth's rotation was not properly accounted for by these authors. Similar extensions have been made by Essawy (1984, 1995). Theoretical treatments based on integral equations aiming at numerical solution for an island of any size have been advanced by Krutitskii (2001) and Martin (2001). Both papers focus on the mathematical foundations without executing explicit computations. Hence quantitative results for physical applications are thus not yet available.

The present work is motivated by recent proposals to construct artificial coastal barriers for harnessing tidal power. Unlike existing schemes based either on using a strong tidal current or building barrages to produce a higher water level in a one- or two-basin reservoir (Baker 2000), the dynamic tidal power (DTP) system initiated by Hulsbergen *et al.* (2005) aims at tides of low or moderate amplitudes, by using an artificially constructed barrier approximately 50 km in length. Several computational models are available for estimating the practical potential. Since the barrier length is much smaller than the typical tidal wavelength, an analytical prediction by matched asymptotics is convenient for the idealized geometry despite the boundary condition (1.1). Here we describe a leading-order theory for tidal diffraction by a small island or cape, and use the predicted coastal runup for the limiting case of a coastal barrier to give a convenient estimate of the available power. We also work out the scattering amplitude in the far field, which may be of interest for environmental considerations.

2. Governing equations of long waves in a rotating sea

We consider a tidal wave of single frequency ω. In a rotating sea of constant depth h, the conservation equations for mass,

$$\mathrm{i}\omega\zeta + h(u_x + v_y) = 0, \tag{2.1}$$

and momentum,

$$\mathrm{i}\omega u - fv = -g\zeta_x, \quad \mathrm{i}\omega v + fu = -g\zeta_y, \tag{2.2a,b}$$

are well known (Proudman 1953), where f is the Coriolis parameter. The time factor $\mathrm{e}^{\mathrm{i}\omega t}$ is assumed but omitted for brevity and is implied from now on.

Equations (2.2) can be solved for the velocity components:

$$k^2 hu = \mathrm{i}\omega\zeta_x + f\zeta_y, \quad k^2 hv = -f\zeta_x + \mathrm{i}\omega\zeta_y, \tag{2.3a,b}$$

where

$$k^2 = \frac{\omega^2 - f^2}{C^2}, \quad C = \sqrt{gh}. \tag{2.4}$$

Substituting (2.3) in (2.1), ζ satisfies the familiar Helmholtz equation:

$$\zeta_{xx} + \zeta_{yy} + k^2\zeta = 0. \tag{2.5}$$

We shall limit this study to the northern hemisphere and diurnal tides, so that $f > 0$, $\omega > f$ and $k^2 > 0$.

3. Elliptic island in open sea

For an elliptic island in the open sea, the full solution for all island sizes can be derived, in principle, by using Mathieu functions (as in Stamnes & Spjelkavik (1995) for classical waves). The task would require elaborate algebra and computations, and is not known to have been carried out. We shall apply the technique of matched asymptotics to derive the approximate solution for a small island. In particular, we aim to find the scattered waves in the far field to complement Proudman's solution in the near field.

3.1. *Outer solution: incident and scattered tides*

Let us define the outer solution ζ valid in the region $kr \geqslant O(1)$ to be the sum of the incident tide ζ^I and the scattered tide ζ^S,

$$\zeta = \zeta^I + \zeta^S, \tag{3.1}$$

where ζ^I is assumed to be a simple Poincaré wave incident at angle θ_i,

$$\zeta^I = A\mathrm{e}^{-\mathrm{i}\boldsymbol{k}\cdot\boldsymbol{x}} = A\mathrm{e}^{\mathrm{i}(\alpha x+\beta y)} = A\mathrm{e}^{-\mathrm{i}kr\cos(\theta-\theta_i)}, \tag{3.2}$$

with $(x, y) = r(\cos\theta, \sin\theta)$ and $(\alpha, \beta) = -k(\cos\theta_i, \sin\theta_i)$. For $\alpha, \beta > 0$, $\pi < \theta_i < 3\pi/2$. Such waves are possible only if $\omega/f > 1$.

Using (2.3), the velocity components of the incident tide are

$$u^I = gA\frac{-\omega\alpha + \mathrm{i}f\beta}{\omega^2 - f^2}\mathrm{e}^{\mathrm{i}(\alpha x+\beta y)}, \quad v^I = gA\frac{-\omega\beta - \mathrm{i}f\alpha}{\omega^2 - f^2}\mathrm{e}^{\mathrm{i}(\alpha x+\beta y)}. \tag{3.3a,b}$$

Suggested by the classical theory of sound around a circular cylinder, the scattered tide ζ^S can be constructed by a series of poles of ascending order:

$$\zeta^S = C_0\mathrm{H}_0(kr) + \sum_{m=1}^{\infty}[C_m\cos m\theta + S_m\sin m\theta]\mathrm{H}_m(kr). \tag{3.4}$$

Throughout this work $\mathrm{H}_m(kr)$ stands for Hankel functions $\mathrm{H}_m^{(2)}(kr)$ for brevity. For general island geometries in a rotating sea, the strengths C_m, S_m, $m = 0, 1, 2, \ldots$, are as yet unknown. For small bodies with size of $O(a)$, the series is expected to be dominated by poles of the first two orders with strengths proportional to $O(k^2a^2)$, i.e.

$$\zeta^S \approx \zeta_0^S + \zeta_1^S, \quad \text{where } \zeta_0^S = C_0\mathrm{H}_0,\ \zeta_1^S = (C_1\cos\theta + S_1\sin\theta)\,\mathrm{H}_1(kr). \tag{3.5}$$

For later asymptotic matching with the inner solution near the small island $r \leqslant O(a)$, we approximate the incident tide for small kr by

$$\frac{\zeta_{in}^I}{A} \approx 1 + \mathrm{i}\alpha x + \mathrm{i}\beta y - \frac{1}{2}(\alpha^2x^2 + \beta^2y^2) - \alpha\beta xy + O(k^3a^3). \tag{3.6}$$

The linear part above corresponds to the irrotational current near the island:

$$u^I_{in} \equiv u^I(0,0) = gA\frac{-\omega\alpha + \mathrm{i}f\beta}{\omega^2 - f^2}, \quad v^I_{in} \equiv v^I(0,0) = gA\frac{-\omega\beta - \mathrm{i}f\alpha}{\omega^2 - f^2}. \tag{3.7a,b}$$

The quadratic part of (3.6) is rotational with the vorticity of order $O(k^2a^2)$, and is needed for determining C_0, as stressed by Martin & Dalrymple (1988) in their matched asymptotic theory of long sound wave scattering by gratings in a non-rotating fluid.

In the far field where $kx, ky, kr \gg 1$, the scattered tide is asymptotically

$$\zeta^S = \zeta^S_0 + \zeta^S_1 \approx C_0\sqrt{\frac{2}{\pi kr}}\mathrm{e}^{-\mathrm{i}(kr-\pi/4)} + (S_1\sin\theta + C_1\cos\theta)\sqrt{\frac{2}{\pi kr}}\mathrm{e}^{-\mathrm{i}(kr-\pi/4-\pi/2)}. \tag{3.8}$$

Using the properties of Hankel functions with small argument, the inner approximation of the scattered tide is

$$\zeta^S = \zeta^S_{0,in} + \zeta^S_{1,in}, \tag{3.9}$$

where the source part is

$$\zeta^S_{0,in} \approx -C_0\frac{2\mathrm{i}}{\pi}\ln\frac{kr}{2} \tag{3.10}$$

and the doublet part is

$$\zeta^S_{1,in} \approx (S_1\sin\theta + C_1\cos\theta)\frac{2\mathrm{i}}{\pi kr} = (S_1 y + C_1 x)\frac{2\mathrm{i}}{\pi kr^2}. \tag{3.11}$$

Use has been made of the relations $\cos\theta = x/r$ and $\sin\theta = y/r$. To determine the pole strengths (C_0, C_1, S_1), we turn to the near-field solution defined in the region $O(k^{-1}) \gg r = O(a)$.

3.2. *The near field (the inner solution η)*

For later determination of the diffraction field, it is convenient to recount Proudman's inner solution. As noted by Rayleigh (Strutt 1897), the governing Helmholtz equation can be approximated by the Laplace equation with an error $O(k^2a^2)$. Hence the inner solution can be found in terms of the complex potential $w(z) = \phi + \mathrm{i}\psi$. To ensure clarity, we denote the near-field surface displacement by $\eta(x, y)$ instead of $\zeta(x, y)$. Proudman (1915) showed first that

$$-g\eta = \mathrm{i}\omega\phi + f\psi, \tag{3.12}$$

which follows by integrating either equation in (2.2) and using Cauchy–Riemann conditions. He then used the classic solution of a current (U, V) passing an elliptical cylinder (see Milne-Thomson 1955, p. 159ff.):

$$w(z) = \frac{1}{2}\left[(U - \mathrm{i}V)\left(z + \sqrt{z^2 - c^2}\right) + (U + \mathrm{i}V)\frac{(a+b)^2}{c^2}\left(z - \sqrt{z^2 - c^2}\right)\right], \tag{3.13}$$

where (a, b) are respectively the major and minor axes of the ellipse,

$$\frac{x^2}{a^2} + \frac{y^2}{b^2} = 1, \tag{3.14}$$

and $c^2 = a^2 - b^2$. By using elliptical coordinates, it can be shown that $\psi = 0$ on the elliptical coast.

For later matching with the far field (outer solution), we seek the outer approximation of $w(z)$ by letting $kr \ll 1$ but $z/c \sim z/a \gg 1$. Since

$$\sqrt{z^2 - c^2} = z - \frac{c^2}{2z} + O\left(\frac{c^4}{z^4}\right), \tag{3.15}$$

the outer approximation of $w(z)$ is

$$\begin{aligned} w_{out} \approx\ & [Ux + Vy + \mathrm{i}(-Vx + Uy)] \\ & - \frac{c^2}{4r^2}[Ux - Vy - \mathrm{i}(Vx + Uy)] + \frac{c^2}{4r^2}\frac{a+b}{a-b}[Ux + Vy + \mathrm{i}(Vx - Uy)]. \end{aligned} \tag{3.16}$$

Separating the real and imaginary parts:

$$\begin{aligned} \phi_{out} &\approx [Ux + Vy] - \frac{c^2}{4r^2}\left[Ux - Vy - \frac{a+b}{a-b}(Ux + Vy)\right] \\ &= [Ux + Vy] - \frac{a+b}{2r^2}[-Ubx - Vay], \end{aligned} \tag{3.17}$$

$$\begin{aligned} \psi_{out} &\approx (-Vx + Uy) + \frac{c^2}{4r^2}\left[(Vx + Uy) + \frac{a+b}{a-b}(Vx - Uy)\right] \\ &= (-Vx + Uy) + \frac{a+b}{2r^2}[Vax - Uby]. \end{aligned} \tag{3.18}$$

The outer approximation of the inner solution η is

$$\begin{aligned} \eta_{out} \approx\ & -\frac{1}{g}(\mathrm{i}\omega\phi_{out} + f\psi_{out}) = -\frac{1}{g}\{(\mathrm{i}\omega U - fV)x + (\mathrm{i}\omega V + fU)y\} \\ & - \frac{1}{g}\left\{\frac{a+b}{2r^2}\left[(\mathrm{i}\omega Ub + fVa)\,x + (\mathrm{i}\omega Va - fUb)\,y\right]\right\}. \end{aligned} \tag{3.19}$$

By equating the coefficients of x and y in (3.19) and (3.6) we obtain

$$U = gA\frac{-\omega\alpha + \mathrm{i}f\beta}{\omega^2 - f^2} = u^I(0,0), \quad V = gA\frac{-\omega\beta - \mathrm{i}f\alpha}{\omega^2 - f^2} = v^I(0,0), \tag{3.20a,b}$$

to the leading order, which agrees with (3.7), as expected.

The inner solution η represented by (3.13) is therefore completely known from the leading-order terms of the far field, and agrees with Proudman (1915). This result will be used to find the strength of the doublet C_1 and S_1 in (3.5) in the outer solution ζ_1^S.

3.3. *Coefficients in the outer solution*

By matching the outer approximation of the inner solution (η_{out}^I, (3.19)) and the inner approximation of the outer solution ($\zeta_{in,1}^S$, (3.11)), we equate the coefficients of x/r^2 and y/r^2, and get, respectively,

$$C_1 = \frac{\mathrm{i}\pi k(a+b)}{4g}(\mathrm{i}\omega Ub + fVa) \tag{3.21}$$

and

$$S_1 = \frac{\mathrm{i}\pi k(a+b)}{4g}(\mathrm{i}\omega Va - fUb). \tag{3.22}$$

Making use of (3.20), we find the doublet strength,

$$C_1 = \frac{\mathrm{i}\pi k(a+b)}{4g}[-\mathrm{i}\alpha(\omega^2 b + f^2 a) - \omega f\beta(a+b)]\frac{gA}{\omega^2 - f^2} \tag{3.23}$$

and

$$S_1 = \frac{\mathrm{i}\pi k(a+b)}{4g}[-\mathrm{i}\beta(\omega^2 a + f^2 b) + \omega f\alpha(a+b)]\frac{gA}{\omega^2 - f^2}. \tag{3.24}$$

With these results, the doublet part ζ_1^S is now complete. Note that U and V hence C_1 and S_1 are fixed by the linear terms in (3.6).

In the limiting case of a thin barrier, $b=0$, and a northward tide, $\alpha=0,\ \ \beta=k$, we get

$$C_1 = \frac{\mathrm{i}\pi ka}{4g}(-f\,Va) = \frac{\mathrm{i}\pi k^2 a^2}{4}\frac{\omega f}{\omega^2 - f^2}A \tag{3.25}$$

and

$$S_1 = \frac{\mathrm{i}\pi k(a)}{4g}(-\mathrm{i}\omega Va) = \frac{\pi k^2 a^2}{4}\frac{\omega^2}{\omega^2 - f^2}A, \tag{3.26}$$

which agrees with Proudman (1915).

As another limiting case, the doublet coefficients for a circular island in a northward incident tide, $\alpha=0,\ \ \beta=k$, are

$$C_1 = \mathrm{i}\pi k^2 a^2 \frac{\omega f}{\omega^2 - f^2}A \quad \text{and} \quad S_1 = -\frac{\pi k^2 a^2}{2}\frac{(\omega^2 + f^2)}{\omega^2 - f^2}A. \tag{3.27a,b}$$

Unlike the doublet strengths, the source strength C_0 in ζ_0^S must be found by considering the second-order approximation of the incident wave in (3.6). This is pointed out by Martin & Dalrymple (1988) in their asymptotic theory of grating scattering. Rayleigh (Strutt 1897) dealt with the same issue in the scattering of aerial and electric waves by reasoning that, without the cylinder, the incident wave would send a certain amount of flow into the cylindrical area. Hence there must be an outward flow from the cylinder to cancel the incoming flux. We shall adopt Rayleigh's more physical reasoning for the elliptic island in a rotating sea.

First let us rewrite (2.3) as

$$k^2 h\,\boldsymbol{u}\cdot\boldsymbol{n} = \mathrm{i}\omega\frac{\partial\zeta}{\partial n} + f\frac{\partial\zeta}{\partial s}, \tag{3.28}$$

where $\boldsymbol{n}$ is the unit normal vector, and n and s are distances along the normal and tangent to a surface. The total (not local) incoming flux of the ambient tide across a closed circle ∂S surrounding the island is

$$k^2 h\oint_{\partial S}\boldsymbol{u}^I\cdot\boldsymbol{n}\,\mathrm{d}s = \mathrm{i}\omega\oint_{\partial S}\frac{\partial\zeta^I}{\partial n}\,\mathrm{d}s + f\oint_{\partial S}\frac{\partial\zeta^I}{\partial s}\,\mathrm{d}s, \tag{3.29}$$

where $\boldsymbol{n}$ points outwards from ∂S. The last integral vanishes. By Gauss's theorem, the incoming flux through ∂S is

$$-\oint_{\partial S} \boldsymbol{u}^I_{in}\cdot\boldsymbol{n}\,\mathrm{d}s=-\frac{\mathrm{i}\omega}{k^2h}\oint_{\partial S}\frac{\partial\zeta^I_{in}}{\partial n}\,\mathrm{d}s=-\frac{\mathrm{i}\omega}{k^2h}\iint_S\nabla^2\zeta^I_{in}\,\mathrm{d}x\,\mathrm{d}y, \tag{3.30}$$

where S is the total area inside ∂S. For small ka, only the quadratic terms in ζ^I contribute:

$$\begin{aligned}\nabla^2\zeta^I_{in} &= A\nabla^2\left(1+\mathrm{i}\alpha x+\mathrm{i}\beta y-\tfrac{1}{2}(\alpha^2x^2+\beta^2y^2)-\alpha\beta xy\right)\\ &= -(\alpha^2+\beta^2)A=-k^2A.\end{aligned} \tag{3.31}$$

Hence the total tidal flux towards the island through ∂S is

$$M_{in}=-\oint_{\partial S}\boldsymbol{u}^I_{in}\cdot\boldsymbol{n}\,\mathrm{d}s=-\frac{\mathrm{i}\omega}{k^2h}\iint_S\nabla^2\zeta^I_{in}\,\mathrm{d}x\,\mathrm{d}y=\frac{\mathrm{i}\omega}{k^2h}k^2\pi abA, \tag{3.32}$$

where πab is the planar area of the elliptic island.

Letting ∂S be a circle at the outer limit of the inner region, $r/a\gg1$, the total outflux repelled by the island is obtained from (3.10) as

$$M_{out}=\frac{\mathrm{i}\omega}{k^2h}2\pi r\frac{\partial\zeta^S_0}{\partial r}\approx\frac{\mathrm{i}\omega}{k^2h}2\pi r\frac{\partial}{\partial r}\left(-C_0\frac{2\mathrm{i}}{\pi}\ln\frac{kr}{2}\right)=\frac{\mathrm{i}\omega}{k^2h}C_0(-4\mathrm{i}). \tag{3.33}$$

Requiring $M_{in}=M_{out}$ we get

$$C_0=\frac{\mathrm{i}\pi k^2ab}{4}A. \tag{3.34}$$

Thus C_0 is the largest for a circular island and zero for a thin barrier. Unlike C_1 and S_1, C_0 is determined by the quadratic terms in (3.6). Hence the scattered source for the elliptic island is

$$\zeta^S_0=\frac{\mathrm{i}\pi k^2ab}{4}A\mathrm{H}_0(kr) \tag{3.35}$$

for all kr and is independent of both the velocity magnitude (U,V) and the direction of the incoming tide, but depends on the Earth's rotation because of (2.4). Moreover, if the island is a thin barrier, $b=0$, the source strength is zero.

In summary, the total wave field for all kr away from the elliptical island is

$$\begin{aligned}\frac{\zeta}{A} &= \mathrm{e}^{-\mathrm{i}\boldsymbol{k}\cdot\boldsymbol{r}}+\frac{\mathrm{i}\pi k^2ab}{4}\mathrm{H}_0(kr)\\ &\quad+\frac{\mathrm{i}\pi k(a+b)}{4}\left[\left([-\mathrm{i}\alpha(\omega^2b+f^2a)-\omega f\beta(a+b)]\frac{1}{\omega^2-f^2}\right)\cos\theta\right.\\ &\quad+\left.\left([-\mathrm{i}\beta(\omega^2a+f^2b)+\omega f\alpha(a+b)]\frac{1}{\omega^2-f^2}\right)\sin\theta\right]\mathrm{H}_1(kr)\\ &\quad+o(k^2a^2),\end{aligned} \tag{3.36}$$

which complements the near-field solution by Proudman (1915). Together with (3.13), the solution is known to $O(k^2a^2)$ everywhere. In appendix A, the above approximate

results will be confirmed by the exact solution for the limiting case of a circular island by Proudman (1915) and Martin (2001).

For large kr, we use the leading approximations for $\mathrm{H}_0^{(2)}(kr)$ and $\mathrm{H}_1^{(2)}(kr)$ and let $(\alpha, \beta) = -k(\cos\theta_i, \sin\theta_i)$ with θ_i being the angle of incidence measured from the positive x axis. The scattered tide can be rewritten as

$$\frac{\zeta_S}{A} = \frac{\mathrm{i}\pi k^2 a^2}{4}\mathcal{A}(\theta)\sqrt{\frac{2}{\pi kr}}\mathrm{e}^{-\mathrm{i}(kr-\pi/4)}, \tag{3.37}$$

where $\mathcal{A}(\theta)$ represents the angular variation of the scattered wave:

$$\begin{aligned}\mathcal{A}(\theta) = {} & \frac{b}{a} - \frac{(1+b/a)}{1-f^2/\omega^2} \\ & \times \left\{\left[\left(\frac{b}{a}+\frac{f^2}{\omega^2}\right)\cos\theta_i - \mathrm{i}\frac{f}{\omega}\left(1+\frac{b}{a}\right)\sin\theta_i\right]\cos\theta \right. \\ & \left. + \left[\left(1+\frac{f^2}{\omega^2}\frac{b}{a}\right)\sin\theta_i + \mathrm{i}\frac{f}{\omega}\left(1+\frac{b}{a}\right)\cos\theta_i\right]\sin\theta\right\}. \end{aligned} \tag{3.38}$$

As a check, in the special limit of $f = 0$ and $b/a = 1$, $\mathcal{A}(\theta)$ reduces to

$$\mathcal{A}(\theta) = 1 - 2\cos(\theta - \theta_i), \tag{3.39}$$

as is known in sound scattering by a circular cylinder (Lamb 1932). In figure 1, polar plots of $|\mathcal{A}(\theta)|$ are shown for $f/\omega = 0.5$, three different angles of incidence $(\pi, 5\pi/4, 3\pi/2)$ and $b/a = 0$, 0.25, 0.50, 0.75 and 1.00, all with the same a. Since the scattering amplitude increases with the planar area of the island, $|\mathcal{A}(\theta)|$ is the smallest for a thin barrier and greatest for a circle. For the sake of comparison, we present in figure 2 the results for the same set of islands in a non-rotating system. In contrast, $|\mathcal{A}(\theta)|$ is relatively larger and never zero in all directions if f is finite.

3.4. *Coastal runup*

Let us now transform (x, y) to elliptical coordinates (μ, ν) defined by

$$z = x + \mathrm{i}y = c\cos(\mu + \mathrm{i}\nu) \quad \text{or} \quad x = c\cosh\mu\cos\nu, \quad y = c\sinh\mu\sin\nu. \tag{3.40a–c}$$

For fixed $\mu = \mu_0$, the point (x, y) is on an ellipse with major and minor axes a and b, where

$$a = c\cosh\mu_0, \quad b = c\sinh\mu_0, \quad a^2 - b^2 = c^2. \tag{3.41a–c}$$

The near-field complex potential can be rewritten as

$$w(\mu + \mathrm{i}\nu) = \phi + \mathrm{i}\psi = U_0(a+b)\cosh(\mu - \mu_0 + \mathrm{i}\nu - \mathrm{i}\theta_i), \tag{3.42}$$

where $U + \mathrm{i}V = \bar{U}\mathrm{e}^{\mathrm{i}\theta_i}$ with U and V given by (3.20). On the ellipse $\mu = \mu_0$,

$$x = a\cos\nu, \quad y = b\sin\nu = \pm b\sqrt{1 - \frac{x^2}{a^2}}, \tag{3.43a,b}$$

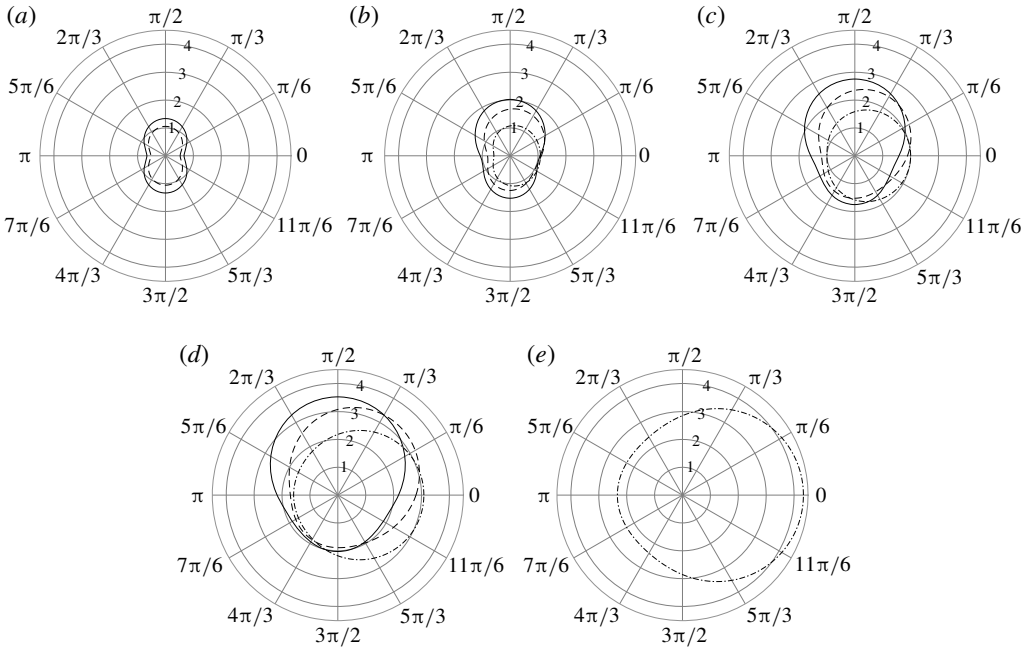

FIGURE 1. Scattering amplitude away from islands of different geometries and incidence angles in a rotating sea with $f/\omega = 0.5$, for $b/a = 0$ (*a*), 0.25 (*b*), 0.50 (*c*), 0.75 (*d*) and 1.00 (*e*). Curves represent $\theta_i = \pi$ (dash–dotted), $\theta_i = 5\pi/4$ (dashed) and $\theta_i = 3\pi/2$ (solid).

the stream function ψ vanishes. The complex potential is

$$\begin{aligned} w(\mu_0 + \mathrm{i}\nu) &= \phi = \bar{U}(a+b)\cosh \mathrm{i}(\nu - \theta_i) = \bar{U}(a+b)\cos(\nu - \theta_i) \\ &= \bar{U}(a+b)\left[\cos\nu\cos\theta_i + \sin\nu\sin\theta_i\right]. \end{aligned} \tag{3.44}$$

In particular, the potential on opposite sides of the ellipse $\left(x, \pm b\sqrt{1 - x^2/a^2}\right)$ is

$$\begin{aligned} \phi_\pm &= \bar{U}(a+b)\left(\cos\nu\cos\theta_i + \sin\nu\sin\theta_i\right) \\ &= \bar{U}(a+b)\left(\frac{x}{a}\cos\theta_i \pm \sqrt{1 - \frac{x^2}{a^2}}\sin\theta_i\right). \end{aligned} \tag{3.45}$$

Hence the water-level difference is

$$\Delta\eta = -\frac{\mathrm{i}\omega}{g}(\phi_+ - \phi_-) = -\frac{2\mathrm{i}\omega\bar{U}\sin\theta_i}{g}(a+b)\sqrt{1 - \frac{x^2}{a^2}}, \tag{3.46}$$

which is the greatest at $x = 0$ and diminishes to zero at $x = \pm a$. Thus, for the same incident tide, the water-level drop is the greatest for a circular island and the smallest for a thin dam. For the same elongated island, the drop is the greatest if the tidal current is normal ($\theta_i a = \pi/2$, $\bar{U}\sin\theta_i = V$), and is zero if it is parallel ($\theta_i = 0$), to the major axis.

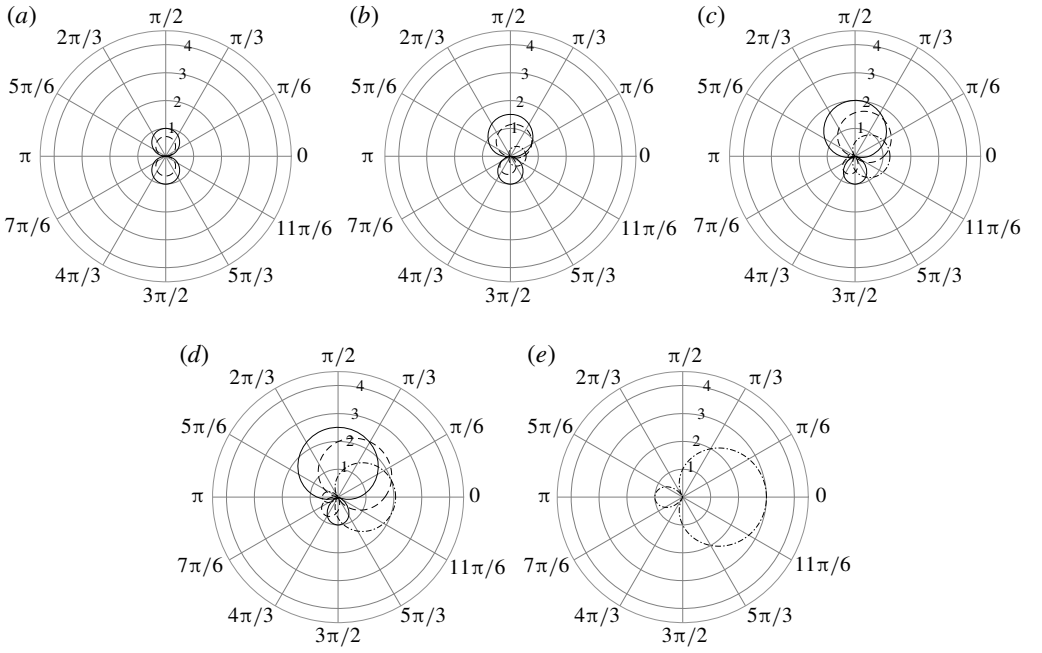

FIGURE 2. Scattering amplitude away from islands of different geometries and incidence angles in a non-rotating fluid ($f = 0$), for $b/a = 0$ (a), 0.25 (b), 0.50 (c), 0.75 (d) and 1.00 (e). Curves represent $\theta_i = \pi$ (dash–dotted), $\theta_i = 5\pi/4$ (dashed) and $\theta_i = 3\pi/2$ (solid).

4. Diffraction by a cape

We now turn to a small semi-elliptic cape perpendicular to a straight coast. Let the sea be in the half-plane $x > 0$ and the long axis of the cape be along the x axis.

4.1. *The incident tide*

Two types of ambient tide will be considered.

4.1.1. *Reflected Poincaré wave*

The surface displacement is

$$\zeta^I = \left(A_I e^{i\alpha x} + A_R e^{-i\alpha x}\right) e^{i\beta y}, \quad \alpha^2 + \beta^2 = k^2, \tag{4.1}$$

where A_I and A_R are, respectively, the amplitudes of incident and reflected tides. To satisfy the no-flux condition on $x = 0$, it is necessary that A_R and A_I are related by

$$A_R = A_I \frac{i\omega\alpha + f\beta}{i\omega\alpha - f\beta}. \tag{4.2}$$

Denoting the total wave amplitude along the coast $x = 0$ by A, then

$$A = A_I \left(1 + \frac{i\omega\alpha + f\beta}{i\omega\alpha - f\beta}\right) = A_I \frac{2i\omega\alpha}{i\omega\alpha - f\beta}. \tag{4.3}$$

The ambient tide can be rewritten as

$$\zeta^I = A\left(\frac{\mathrm{i}\omega\alpha - f\beta}{2\mathrm{i}\omega\alpha}\mathrm{e}^{\mathrm{i}\alpha x} + \frac{\mathrm{i}\omega\alpha + f\beta}{2\mathrm{i}\omega\alpha}\mathrm{e}^{-\mathrm{i}\alpha x}\right)\mathrm{e}^{\mathrm{i}\beta y}. \tag{4.4}$$

From (4.4), the velocity components can be found by using (2.3).

For later matching with the near field, the inner approximation of ζ^I for $kr \ll 1$ is

$$\frac{\zeta^I_{in}}{A} = 1 - \frac{f\beta}{\omega}x + \mathrm{i}\beta y - \frac{1}{2}(\alpha^2x^2 + \beta^2y^2) - \mathrm{i}\frac{f}{\omega}\beta^2xy + O(k^3a^3). \tag{4.5}$$

Again, both linear and quadratic terms are kept in (4.5) for later determination of the scattered wave in the outer field.

Corresponding to the linear terms above, the leading-order inner approximation of the incoming current near the cape is

$$u^I(0,0) \approx 0, \quad v^I(0,0) \approx -\frac{gA\beta}{\omega}. \tag{4.6a,b}$$

Thus the tidal current is essentially parallel to the coast.

4.1.2. *Kelvin wave*

Propagating along the coast, the Kelvin wave is given by

$$\zeta^I = A\mathrm{e}^{(-fx+\mathrm{i}\omega y)/C}, \tag{4.7}$$

with $C = \sqrt{gh}$. In the near field, $kr \ll 1$,

$$\zeta^I_{in} \approx A\left[1 - \frac{fx}{C} + \frac{\mathrm{i}\omega y}{C} + \frac{1}{2C^2}\left(f^2x^2 - \omega^2y^2\right) - \mathrm{i}\frac{f}{\omega}\beta^2xy + O(k^3a^3) + \cdots\right]. \tag{4.8}$$

The corresponding tidal current has the components

$$u^I_{in} \approx 0 \quad \text{and} \quad v^I_{in} \approx -\frac{A}{h}\sqrt{gh} = \text{const.} \tag{4.9a,b}$$

and is parallel to the coast.

4.2. *The outer solution*

In his theory of tidal diffraction by a coastal estuary, Buchwald (1971) derived by Fourier transform the Green's function which represents a point source at the origin. To account for the scattering effects of a small island, we approximate the scattered wave by the sum of a source and a doublet,

$$\zeta \approx \zeta^I + C_0G + D\frac{\partial G}{\partial y}, \tag{4.10}$$

where C_0 and D are the unknown strengths of the source and doublet, respectively. We have replaced Buchwald's Green's function ζ_G by G defined by $\zeta_G = (\omega/2g)G$. It can be shown that the need for $\partial G/\partial x$ does not arise. Buchwald has given the approximations of G valid for both the far field $kr \gg 1$ and the near field $kr \ll 1$ and for both $\sigma = \omega/f > 1$ and $\sigma = \omega/f < 1$. We shall focus our discussion on diurnal tides and the northern hemisphere with $\sigma = \omega/f > 1$.

4.2.1. *The far field* ($kr \gg 1$)

For $\omega > f$, Buchwald has derived the far field of the source to be

$$G \approx G_K \mathrm{H}(\theta_0 - \theta) + G_P, \tag{4.11}$$

where $\mathrm{H}(\theta_0 - \theta)$ denotes the Heaviside function with

$$\theta_0 = -\sin^{-1}(kC/\omega) = -\sin\sqrt{1 - \frac{f^2}{\omega^2}}, \tag{4.12}$$

G_K is the Kelvin wave given by

$$G_K = \frac{2f}{\omega} \mathrm{e}^{(\mathrm{i}\omega y - fx)/C} \tag{4.13}$$

and G_P denotes the Poincaré wave

$$G_P = \frac{\omega^2 - f^2}{\omega^2} \left(\frac{2}{\pi kr}\right)^{1/2} \frac{\cos\theta}{\cos\theta - \mathrm{i}(f/\omega)\sin\theta} \mathrm{e}^{-\mathrm{i}(kr - \pi/4)} + O((kr)^{-3/2}), \tag{4.14}$$

where (r, θ) are the polar coordinates.

Since

$$\frac{\partial}{\partial y} = \sin\theta \frac{\partial}{\partial r} + \frac{\cos\theta}{r} \frac{\partial}{\partial \theta} = \frac{y}{r} \frac{\partial}{\partial r} + \frac{x}{r^2} \frac{\partial}{\partial \theta}, \tag{4.15}$$

the far field of the doublet is

$$\begin{aligned} D\frac{\partial G}{\partial y} \approx D \Bigg\{ & 2\mathrm{i}f \mathrm{e}^{(\mathrm{i}\omega y - fx)/C} \mathrm{H}(\theta_0 - \theta) \\ & - \mathrm{i}k \frac{\omega^2 - f^2}{\omega^2} \sqrt{\frac{2}{\pi kr}} \frac{y}{r} \frac{\cos\theta}{\cos\theta - \mathrm{i}(f/\omega)\sin\theta} \mathrm{e}^{-\mathrm{i}(kr - \pi/4)} \Bigg\} + O(kr)^{-3/2}. \end{aligned} \tag{4.16}$$

The total scattered wave in the outer field is

$$\begin{aligned} \zeta^S \approx & \left(C_0 \frac{2f}{\omega} + D\frac{2\mathrm{i}f}{C}\right) \mathrm{e}^{(\mathrm{i}\omega y - fx)/C} \mathrm{H}(\theta_0 - \theta) \\ & + (C_0 - \mathrm{i}kD\sin\theta) \left\{ \frac{\omega^2 - f^2}{\omega^2} \sqrt{\frac{2}{\pi kr}} \frac{\cos\theta}{\cos\theta - \mathrm{i}(f/\omega)\sin\theta} \mathrm{e}^{-\mathrm{i}(kr - \pi/4)} \right\}. \end{aligned} \tag{4.17}$$

The physics is an extension to that described by Buchwald. In particular, $\theta_0 \to -\pi/2$ for $f/\omega \to 1$; no Kelvin wave is produced. On the other hand, $\theta_0 \to 0$ if $f/\omega \to 1$ from below; a Kelvin wave is present for all $y < 0$. The intensity of the Poincaré wave varies with direction differently, being the weakest in directions parallel and normal to the coast ($\theta = 0, \pm\pi/2$), and strongest along $\theta = \pm\pi/4$.

The coefficients C_0 and D will now be determined by matching the small-kr approximation of the outer solution (the wave field) with the large-z/a approximation of the near field.

For matching with the inner solution, we need only the following inner approximations given by Buchwald (1971). Focusing on $\omega > f$ only,

$$G \approx \frac{\omega}{2g} \left[1 - \frac{2\mathrm{i}}{\pi} \log\frac{\gamma kr}{2} - \frac{1}{\pi\sigma} \left(2\theta + \mathrm{i}\log\frac{\sigma + 1}{\sigma - 1}\right)\right] + O(kr), \quad \sigma = \frac{\omega}{f}. \tag{4.18}$$

It is easy to find for $kr \ll 1$ that

$$\frac{\partial G}{\partial y} \approx \left\{ \sin\theta \left(-\frac{2\mathrm{i}}{\pi r} \right) + \frac{\cos\theta}{r} \left(\frac{-2}{\pi\sigma} \right) \right\} = -\frac{2\mathrm{i}}{\pi} \frac{y}{r^2} - \frac{2}{\pi\sigma} \frac{x}{r^2}. \tag{4.19}$$

The inner approximation of the outer solution is, for the incident and reflected Poincaré wave,

$$\begin{aligned} \zeta &\approx \zeta^I + C_0 G + D \frac{\partial G}{\partial y} \\ &\approx A + \frac{\beta A}{\omega} (\mathrm{i}\omega y - fx) \\ &\quad + C_0 \left(1 - \frac{2\mathrm{i}}{\pi} \log \frac{\gamma kr}{2} \right) + D \left\{ -\frac{2\mathrm{i}}{\pi} \frac{y}{r^2} - \frac{2}{\pi\sigma} \frac{x}{r^2} \right\}, \quad kr \ll 1, \end{aligned} \tag{4.20}$$

and for the Kelvin tide,

$$\begin{aligned} \zeta &\approx \zeta^I + C_0 G + D \frac{\partial G}{\partial y} \\ &\approx A - A \frac{f}{\sqrt{gh}} x + A \frac{\mathrm{i}\omega}{\sqrt{gh}} y \\ &\quad + C_0 \left(1 - \frac{2\mathrm{i}}{\pi} \log \frac{\gamma kr}{2} \right) + D \left\{ -\frac{2\mathrm{i}}{\pi} \frac{y}{r^2} - \frac{2}{\pi\sigma} \frac{x}{r^2} \right\}, \quad kr \ll 1. \end{aligned} \tag{4.21}$$

4.3. *Matching with the near field*

The near field (inner solution, again denoted by η) can be obtained from § 3.2 by taking $U = 0$ and $V \neq 0$ in (4.6) or (4.9).

In particular, the outer approximation of the inner solution η is

$$\begin{aligned} \eta_{out} &= -\frac{1}{g} (\mathrm{i}\omega\phi + f\psi)_{out} \\ &= -\frac{1}{g} \{ -f\,Vx + \mathrm{i}\omega Vy \} - \frac{1}{g} \frac{Va(a+b)}{2r^2} (fx + \mathrm{i}\omega y), \quad \frac{r}{c} \gg 1. \end{aligned} \tag{4.22}$$

4.3.1. *Reflected Poincaré tide*

For the reflected Poincaré tide, we match the coefficients of x in (4.22) and (4.20):

$$\frac{fV}{g} = -f \frac{\beta A}{\omega}, \quad \text{hence} \quad V = -\frac{g\beta A}{\omega}, \tag{4.23}$$

as in (4.6). The same result is obtained by matching the coefficients of y in the same equations.

Matching the coefficients of x/r^2,

$$-\frac{1}{g} \frac{Va(a+b)}{2} f = -\frac{2f}{\pi\omega} D, \tag{4.24}$$

and the coefficients of y/r^2,

$$-\frac{1}{g} \frac{Va(a+b)}{2} \mathrm{i}\omega = -D \frac{2\mathrm{i}}{\pi}, \tag{4.25}$$

we get the same doublet strength:

$$D=\frac{\omega}{4g}\pi a(a+b)V=-\frac{\omega}{4g}\pi a(a+b)\frac{g\beta A}{\omega}=-\frac{\pi ka(a+b)}{4}\frac{\beta}{k}A. \tag{4.26}$$

4.3.2. *Kelvin tide*

For the Kelvin tide, matching the coefficients of x and y in (4.22) and (4.21) gives

$$\frac{fV}{g}=-\frac{fA}{\sqrt{gh}}\quad\text{and}\quad-\frac{\mathrm{i}\omega V}{g}=\frac{\mathrm{i}\omega A}{\sqrt{gh}}, \tag{4.27a,b}$$

which leads to the same result,

$$V=-\frac{gA}{\sqrt{gh}}. \tag{4.28}$$

Matching the coefficients of x/r^2 or y/r^2 gives

$$-\frac{Df}{\pi g}=-\frac{fVa(a+b)}{2g},\quad -D\frac{2\mathrm{i}}{\pi}=-\mathrm{i}\omega V\frac{a(a+b)}{2g}, \tag{4.29a,b}$$

which gives the same result for D. Since $V=-gA/\sqrt{gh}=-gA/C$, we have

$$D=\frac{\pi\omega Va(a+b)}{4g}=-\frac{\pi ka(a+b)}{4}A\frac{\omega}{kC}. \tag{4.30}$$

Thus the doublet strength is different from (4.26).

4.4. *The source strength* C_0

We invoke Rayleigh's argument by finding first the tide influx repelled by the cape. Let ∂S be a semicircle surrounding the cape. By using the orthogonal elliptic coordinates μ, ν defined by $x+\mathrm{i}y=c\cos(\mu+\mathrm{i}\nu)$, it is shown in appendix B that (3.29) is equivalent to

$$k^2h\int_{\partial S}\boldsymbol{u}_{in}^I\cdot\boldsymbol{n}\,\mathrm{d}s=\mathrm{i}\omega\int_{\partial S}\frac{\partial\zeta_{in}^I}{\partial\mu}\,\mathrm{d}\nu+f\int_{\partial S}\frac{\partial\zeta_{in}^I}{\partial\nu}\,\mathrm{d}\nu. \tag{4.31}$$

The line integrals above must be evaluated for Poincaré tide and Kelvin tide by using the quadratic part $\zeta_{in,2}^I$ in (4.5) and (4.8), respectively, for ζ_{in}^I.

4.4.1. *Reflected Poincaré tide*

From (4.5), the second-order part of ζ_{in}^I is

$$\begin{aligned}\zeta_{in,2}^I &= -\frac{A}{2}c^2(\alpha^2\cosh^2\mu\cos^2\nu+\beta^2\sinh^2\mu\sin^2\nu)\\ &\quad-\mathrm{i}A\frac{f}{\omega}\beta^2c^2\cosh\mu\cosh\nu\sinh\mu\sin\nu\\ &= -\frac{A}{2}c^2(\alpha^2\cosh^2\mu\cos^2\nu+\beta^2\sinh^2\mu\sin^2\nu)-\mathrm{i}A\frac{f}{4\omega}\beta^2c^2\sinh 2\mu\sin 2\nu.\end{aligned} \tag{4.32}$$

Referring to (4.31), we get, on the ellipse, $\mu = \mu_0$,

$$\begin{aligned}\int_{-\pi/2}^{\pi/2} \mathrm{d}\nu\, \frac{\partial \zeta^I_{in,2}}{\partial \mu} &= -Ac^2 \cosh\mu_0 \sinh\mu_0 \int_{-\pi/2}^{\pi/2} \mathrm{d}\nu\, (\alpha^2 \cos^2\nu + \beta^2 \sin^2\nu) \\ &\quad - \mathrm{i}A\frac{f}{2\omega}\beta^2 c^2 \cosh 2\mu_0 \int_{-\pi/2}^{\pi/2} \sin 2\nu\, \mathrm{d}\gamma \\ &= -Aab\left[\alpha^2\left(\frac{\nu}{2} - \frac{\sin 2\nu}{4}\right) + \beta^2\left(\frac{\nu}{2} + \frac{\sin 2\nu}{4}\right)\right]_{-\pi/2}^{\pi/2} \\ &= -Aab(\alpha^2+\beta^2)\frac{\pi}{2} = -A\frac{\pi k^2 ab}{2}, \end{aligned} \tag{4.33}$$

$$\begin{aligned}\int_{-\pi/2}^{\pi/2} \mathrm{d}\nu\, \frac{\partial \zeta^I_{in,2}}{\partial \nu} &= A(\alpha^2\cosh^2\mu - \beta^2\sinh^2\mu)\int_{-\pi/2}^{\pi/2} \mathrm{d}\nu\, \frac{1}{2}\sin 2\nu \\ &= \frac{A}{4}A(\alpha^2\cosh^2\mu - \beta^2\sinh^2\mu)[\cos 2\nu]_{-\pi/2}^{\pi/2} = 0. \end{aligned} \tag{4.34}$$

Hence the flux that the incoming tide pushes towards the cape is

$$M_{in} = -\frac{\mathrm{i}\omega}{k^2 h}\int_{-\pi/2}^{\pi/2} \mathrm{d}\nu\, \frac{\partial \zeta^I_{in,2}}{\partial \mu} = \frac{\mathrm{i}\omega}{k^2 h}\frac{\pi A k^2 ab}{2}. \tag{4.35}$$

Across a semicircle at the outer limit of the inner region, $r/a \gg 1$, the total repelling flux is, from (4.20),

$$M_{out} = \frac{\mathrm{i}\omega}{k^2 h}\pi r\frac{\partial \zeta_0^S}{\partial r} \approx \frac{\mathrm{i}\omega}{k^2 h}\pi r\frac{\partial}{\partial r}\left(C_0 - C_0\frac{2\mathrm{i}}{\pi}\ln\frac{kr}{2}\right) = -\frac{\mathrm{i}\omega}{k^2 h}C_0\frac{2\mathrm{i}\omega}{2g}, \tag{4.36}$$

which is one-half of (3.33). It follows by requiring $M_{in} = M_{out}$ that

$$C_0 = \frac{\mathrm{i}A}{4}\pi k^2 ab. \tag{4.37}$$

Again, C_0 is the largest for a circle ($b = a$) and zero for a thin barrier ($b = 0$).

In summary the outer tidal field is given by (4.10) with the ambient tide given by (4.4), the source strength by (4.37) and the doublet strength by (4.26).

4.4.2. *Kelvin tide*

For the Kelvin tide incident from the north, $\beta = 0$, the second-order part is, from (4.8),

$$\zeta^I_{in,2} = \frac{A}{2C^2}\left(f^2x^2 - \omega^2 y^2\right) = \frac{Ac^2}{2C^2}\left(f^2\cosh^2\mu\cos^2\nu - \omega^2\sinh^2\mu\sin^2\nu\right). \tag{4.38}$$

On the semi-ellipse, $\mu = \mu_0$,

$$\begin{aligned}\int_{-\pi/2}^{\pi/2} \mathrm{d}\nu\, \frac{\partial \zeta_2^I}{\partial \mu} &= \int_{-\pi/2}^{\pi/2} \mathrm{d}\nu\, \frac{Ac^2}{C^2}\sinh\mu_0\cosh\mu_0(f^2\cos^2\nu - \omega^2\sin^2\nu) \\ &= -\frac{A}{2C^2}\pi ab(\omega^2 - f^2) = -\frac{A}{2}\pi k^2 ab \end{aligned} \tag{4.39}$$

and

$$\int_{-\pi/2}^{\pi/2} \mathrm{d}\nu \, \frac{\partial \zeta_2^I}{\partial \nu} = -\frac{1}{2}\frac{Ac^2}{gh}(\omega^2 \sinh^2 \mu_0 - f^2 \cosh^2 \mu_0) \int_{-\pi/2}^{\pi/2} \mathrm{d}\nu \, \sin 2\nu = 0. \tag{4.40}$$

Again

$$\frac{\mathrm{i}\omega}{k^2 h}\frac{A}{2}\pi k^2 ab = M_{in}. \tag{4.41}$$

From (4.21), the outflux through a semicircle is still given by (4.36). Upon equating the influx and and outflux, we get

$$C_0 = \frac{\mathrm{i}A}{4}\pi k^2 ab. \tag{4.42}$$

In summary, the outer tidal field is given by (4.10) with the ambient tide given by (4.7), the source strength by (4.42) and the doublet strength by (4.30). The two ambient waves lead to the same source strength but different doublet strengths.

4.5. *Scattered wave pattern in the far field*

We summarize below the scattering amplitudes for the two incident tides.

4.5.1. *Incident Poincaré tide*

Using (4.26) and (4.37), we get

$$\begin{aligned} C_0\frac{2f}{\omega} + D\frac{2\mathrm{i}f}{C} &= \mathrm{i}A\frac{f}{\omega}\frac{\pi k^2 ab}{2} - \mathrm{i}A\frac{f}{kC}\frac{\pi k^2 a(a+b)}{2}\frac{\beta}{k} \\ &= \frac{\mathrm{i}A\pi k^2 a^2}{2}\frac{f}{\omega}\left[\frac{b}{a} - \frac{\omega}{kC}\frac{\beta}{k}\left(1+\frac{b}{a}\right)\right]. \end{aligned} \tag{4.43}$$

Let us define the directional factor of the scattered Kelvin wave by

$$\mathcal{A}_{KP} = \frac{f}{\omega}\left\{\frac{b}{a} - \frac{\omega}{kC}\frac{\beta}{k}\left(1+\frac{b}{a}\right)\right\} = \frac{f}{\omega}\left\{\frac{b}{a} + \frac{\sin\theta_i}{\sqrt{1-f^2/\omega^2}}\left(1+\frac{b}{a}\right)\right\}. \tag{4.44}$$

Since

$$\begin{aligned} C_0 - \mathrm{i}kD\sin\theta &= \frac{\mathrm{i}A\pi k^2 ab}{4} - \mathrm{i}k\frac{-\pi ka(a+b)}{4}\frac{\beta}{k}A\sin\theta \\ &= \frac{\mathrm{i}A\pi k^2 a^2}{4}\left[\frac{b}{a} - \left(1+\frac{b}{a}\right)\sin\theta_i \sin\theta\right], \end{aligned} \tag{4.45}$$

the amplitude of the scattered Poincaré wave is

$$\begin{aligned} &\frac{\mathrm{i}A\pi k^2 a^2}{4}\frac{\omega^2 - f^2}{\omega^2}\left[\frac{b}{a} - \left(1+\frac{b}{a}\right)\sin\theta_i\sin\theta\right]\frac{\cos\theta}{\cos\theta - \mathrm{i}(f/\omega)\sin\theta_i\sin\theta} \\ &= \frac{\mathrm{i}A\pi k^2 a^2}{4}\mathcal{A}_{PP}, \end{aligned} \tag{4.46}$$

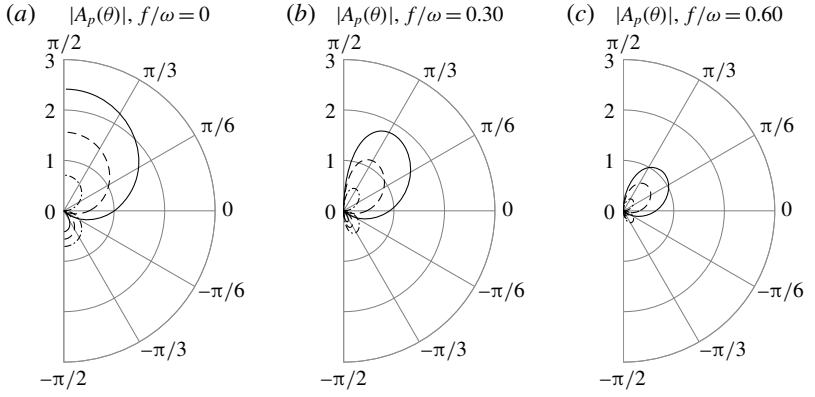

FIGURE 3. Directional pattern of scattered Poincaré wave $|\mathcal{A}_{PP}|$ for a cape, for $f/\omega = 0$ (*a*), 0.30 (*b*) and 0.60 (*c*). Direction of incident Poincaré wave: $\theta_i = 5\pi/4$. Curves represent $b/a = 0$ (dash–dotted), $b/a = 0.50$ (dashed) and $b/a = 1.00$ (solid).

where

$$\mathcal{A}_{PP}(\theta) = \left(1 - \frac{f^2}{\omega^2}\right)\left[\frac{b}{a} - \left(1 + \frac{b}{a}\right)\sin\theta_i \sin\theta\right] \frac{\cos\theta}{\cos\theta - \mathrm{i}(f/\omega)\sin\theta} \tag{4.47}$$

represents the directional pattern of the scattered Poincaré wave. The magnitude

$$|\mathcal{A}_{PP}(\theta)| = \left(1 - \frac{f^2}{\omega^2}\right)\left[\frac{b}{a} - \left(1 + \frac{b}{a}\right)\sin\theta_i \sin\theta\right] \frac{\cos\theta}{\sqrt{\cos^2\theta + (f^2/\omega^2)\sin^2\theta}} \tag{4.48}$$

is larger for smaller f/ω.

We display the numerical results for $|\mathcal{A}_{PP}(\theta)|$ in figure 3 for $\theta_i = 5\pi/4$ and for several different f/ω and b/a. While the extrema are at $\theta = \pm\pi/2$ for $f/\omega = 0$, they are shifted to $\theta = \pm\pi/4$.

4.5.2. *Kelvin tide*

Using (4.42) and (4.30), the amplitude of the scattered Kelvin wave is

$$\begin{aligned} C_0\left(\frac{2f}{\omega}\right) + D\left(\frac{2\mathrm{i}f}{C}\right) &= \frac{\mathrm{i}A\pi k^2 ab}{4}\left(\frac{2f}{\omega}\right) - \frac{\pi k^2 a(a+b)}{4}\frac{\omega}{kC}A\left(\frac{2\mathrm{i}f}{\omega}\right) \\ &= \frac{\mathrm{i}A\pi k^2 a^2}{2}\frac{f}{\omega}\left[\frac{b}{a} - \frac{\omega}{kC}\left(1 + \frac{b}{a}\right)\right] = \mathrm{i}\frac{\mathrm{i}A\pi k^2 a^2}{2}\mathcal{A}_{KK}, \end{aligned} \tag{4.49}$$

where the factor

$$\mathcal{A}_{KK} = \frac{f}{\omega}\left[\frac{b}{a} - \frac{\omega}{kC}\left(1 + \frac{b}{a}\right)\right] = \frac{f}{\omega}\left[\frac{b}{a} - \frac{1}{\sqrt{1 - f^2/\omega^2}}\left(1 + \frac{b}{a}\right)\right] \tag{4.50}$$

gives the dependence of the scattered Kelvin wave on the island shape. It is virtually the same as (4.44) except for the factor θ_i.

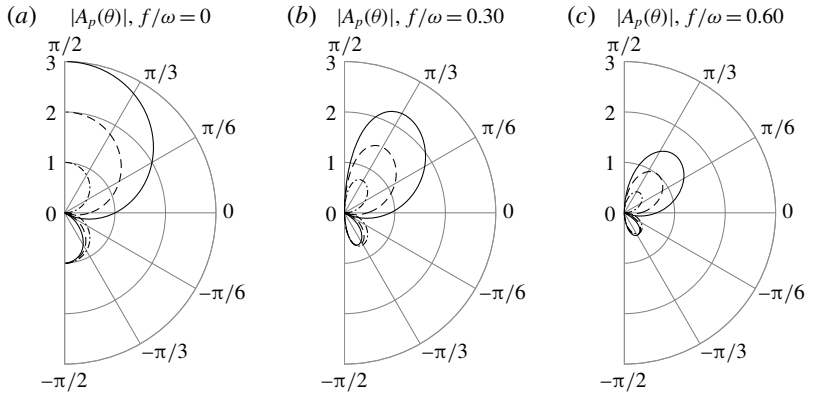

FIGURE 4. Directional pattern of scattered Poincaré wave for a cape due to incident Kelvin wave, for $f/\omega = 0$ (*a*), 0.30 (*b*) and 0.60 (*c*). Curves represent $b/a = 0.0$ (dash–dotted), $b/a = 0.5$ (dashed) and $b/a = 1.0$ (solid).

On the other hand,

$$C_0 - \mathrm{i}kD\sin\theta = \frac{\mathrm{i}A\pi k^2 ab}{4} - \mathrm{i}k\frac{-\pi ka(a+b)}{4}\frac{\omega}{kC}\sin\theta$$
$$= \frac{\mathrm{i}A\pi k^2 a^2}{4}\left[\frac{b}{a} + \left(1+\frac{b}{a}\right)\frac{\omega}{kC}\sin\theta\right]. \tag{4.51}$$

The amplitude of the scattered Poincaré wave is

$$\frac{\mathrm{i}A\pi k^2 a^2}{4}\frac{\omega^2 - f^2}{\omega^2}\left[\frac{b}{a} + \left(1+\frac{b}{a}\right)\frac{\omega}{kC}\sin\theta\right]\frac{\cos\theta}{\cos\theta - \mathrm{i}(f/\omega)\sin\theta}$$
$$= \frac{\mathrm{i}A\pi k^2 a^2}{4}\mathcal{A}_{PK}(\theta), \tag{4.52}$$

where

$$\mathcal{A}_{PK}(\theta) = \frac{\omega^2 - f^2}{\omega^2}\left[\frac{b}{a} + \left(1+\frac{b}{a}\right)\frac{\omega}{kC}\sin\theta\right]\frac{\cos\theta}{\cos\theta - \mathrm{i}(f/\omega)\sin\theta}$$
$$= \left(1 - \frac{f^2}{\omega^2}\right)\left[\frac{b}{a} + \left(1+\frac{b}{a}\right)\frac{\sin\theta}{\sqrt{1-(f^2/\omega^2)}}\right]\frac{\cos\theta}{\cos\theta - \mathrm{i}(f/\omega)\sin\theta} \tag{4.53}$$

is the directional factor of the scattered Poincaré wave. The magnitude of this factor depends parametrically on b/a and is larger for smaller f/ω.

Sample results for the directional pattern $|\mathcal{A}_{PK}|$ are shown in figure 4, which are quite similar to those for $|\mathcal{A}_{PP}|$ in figure 3. In the plot for $f/\omega = 0$, the curve for $b/a = 1$ agrees with that for sound scattering by a rigid circular cylinder.

We now turn to an application in technology.

5. Harnessing tidal power from a coast-connected dam

During 2005–08, Hulsbergen and colleagues proposed the new scheme that they called dynamic tidal power (DTP) to harness energy from tides (Hulsbergen *et al.* 2005, 2008*a*,*b*). The initial idea is to construct a long dam protruding perpendicularly

from a straight coast, so that the difference in water levels on the two sides of the dam can be used to drive a linear array of turbines distributed along the dam. It was hoped that 10 GW of electricity could be harvested from a dam of 40 km length with 2000 turbines of 5 MW capacity each. (For a video introduction, see https://www.dutchmarineenergy.com/dutch-concepts/dtp.) Interest in DTP has prompted several elaborate computational studies in The Netherlands, China and Korea for various sites and dam geometries (see e.g. Klopman 2003; Liu & Zhang 2014; Dai, Zhang & Zheng 2017; Dai *et al.* 2018). For the simplest geometry of a thin dam orthogonal to a straight coast (the I dam), Mei (2012) has derived an analytical theory of tidal diffraction and an explicit formula for the head difference. A quantitative estimate accounting for both the spatial variation and transient flow is made here for its power potential.

The water-level difference across a thin dam of length a is given by (3.46) with $U_0 \sin\theta_0 = V,\ b = 0$,

$$\mathrm{Re}(\Delta\eta(x,t)) = \begin{cases} \mathrm{Re}\left(-\dfrac{2\mathrm{i}\omega Va}{g}\sqrt{1-\dfrac{x^2}{a^2}}\,\mathrm{e}^{\mathrm{i}\omega t}\right), & 0<x<a, \\ 0, & x>a, \end{cases} \tag{5.1}$$

where V is the maximum tidal velocity at $x=0$ in the absence of the dam,

$$V = \begin{cases} -\dfrac{g\beta A}{\omega}, & \text{reflected Poincaré tide}, \\ -\dfrac{gA}{\sqrt{gh}}, & \text{Kelvin tide}. \end{cases} \tag{5.2}$$

Let the spacing between two adjacent turbines be ℓ, and the total number of turbines be $N = a/\ell$, i.e. $a = N\ell$. The centres of the turbine tunnels are at $x_n = n\ell, \quad n = 0, 1, 2, \ldots, N$. The head difference across nth turbine at $x_n = n\ell$ is

$$\Delta\eta_n(t) = |\Delta\eta_0|\left(1-\frac{n^2}{N^2}\right)^{1/2}\cos\omega\tau, \quad \omega\tau \equiv \omega t - \pi/2, \tag{5.3}$$

where

$$|\Delta\eta_0| = \frac{2\omega Va}{g} \tag{5.4}$$

is the maximum $|\Delta\eta_n|$ at $x=0$. Let each turbine be housed in a tunnel of radius R. By Toricelli's law the water speed through the nth turbine tunnel is estimated as $C_d\sqrt{2g|\Delta\eta_n(\tau)|}\,\mathrm{sgn}(\Delta\eta_n(\tau))$, where C_d is the discharge coefficient. The discharge rate is, in $\mathrm{m}^3\ \mathrm{s}^{-1}$,

$$\begin{aligned} Q_n &= C_d\pi R^2\sqrt{2g\Delta\eta_n(t)}\,\mathrm{sgn}(\Delta\eta_n(\tau)) \\ &= C_d\pi R^2\sqrt{2g|\Delta\eta_0|}(N^2-n^2)^{1/4}\sqrt{|\cos\omega\tau|}\,\mathrm{sgn}(\cos\omega\tau). \end{aligned} \tag{5.5}$$

Let the efficiency of the turbine be C_e. The time average of $\rho g\Delta\eta_n(\tau)$ and $Q_n(\tau)$ gives a rough estimate of the power output from turbine n:

$$\begin{aligned} P_n &= C_eC_d(\rho g\,\overline{Q_n\Delta\eta_n}) \\ &= C_eC_d\rho g\pi R^2\sqrt{2g}|\Delta\eta_0|^{3/2}\left(1-\frac{n^2}{N^2}\right)^{3/4}\overline{|\cos^{3/2}\omega\tau|}. \end{aligned} \tag{5.6}$$

Since $\cos(-t') = \cos t'$,

$$\overline{|\cos^{3/2}\omega\tau|} = \frac{\omega}{2\pi}\int_0^{2\pi/\omega} |\cos\omega\tau|^{3/2}\,\mathrm{d}\tau = \frac{4}{2\pi}\int_0^{\pi/2}\cos^{3/2}t'\,\mathrm{d}t' = 0.5564. \tag{5.7}$$

Use is made of the identity

$$\int_0^{\pi/2}\cos^{3/2}t'\,\mathrm{d}t' = \frac{1}{6\sqrt{2\pi}}\left[\Gamma\left(\frac{1}{4}\right)\right]^2 = \frac{(3.62561)^2}{6\sqrt{2\pi}} = 0.87401 \tag{5.8}$$

Gradshteyn & Rizhik (1980, p. 369). Thus the power output from turbine n is

$$P_n = 0.5564(C_eC_d)\rho g\pi R^2\sqrt{2g}|\Delta\eta_0|^{3/2}\left(1-\frac{n^2}{N^2}\right)^{3/4}. \tag{5.9}$$

The total power output from N turbines along a cape is, therefore,

$$P = \sum_{n=0}^{N} P_n = 0.5564C_eC_dM|\Delta\eta_0|^{3/2}\Sigma_N, \tag{5.10}$$

where

$$M = \rho g\pi R^2\sqrt{2g}, \quad \Sigma_N = \sum_{n=0}^{N}\left(1-\frac{n^2}{N^2}\right)^{3/4}. \tag{5.11a,b}$$

Consider, for illustration, a thin dam with $b = 0$ in a shallow sea of depth 30 m. We take $\rho = 10^3$ kg m^{-3}, $g = 9.8$ m s^{-2}, $\omega = 2\pi/12$ h^{-1} and $R = 4$ m, so that $\pi R^2 = 50.265$ m^2. For turbine spacing of $\ell = 20$ m and dam length $a = 20, 30, 40, 50$ km, the total number of turbines is $N = 1000, 1500, 2000, 2500$, respectively. At present, no empirical data on turbine tunnel loss exists, and therefore the coefficients C_e and C_d can only be speculated. In a numerical simulation of a proposed tidal barrier in the Severn Estuary, Bristol Channel, UK, Zhou, Falconer & Lin (2014) assumed $C_e = C_d = 1$ and obtained satisfactory agreement with measured data. In the following numerical examples $C_eC_d = 1.0$ is assumed tentatively for preliminary estimates. In table 1, the calculated water-level difference and estimated power output are listed for $V = 1$ and 2 m s^{-1}. The corresponding range of an incident Kelvin tide is $2A = 3.5$ and 7.0 m, lower than the tidal range of $2A \approx 13$ m in the Bay of Fundy, Canada. For other tidal currents, P is proportional to $|\Delta\eta_0|^{3/2} \propto V^{3/2}$. For comparison, the average capacity of a nuclear power plant is 0.5 GW. The maximum power output in the Bay of Fundy is 2.5 GW. The predictions here are encouraging, though the appropriate values of C_e and C_d must await further experimental verification.

As the construction of a new dam near the coast not only will be expensive but also will likely face strong environmental objections by coastal communities, the alternative to find an existing cape (or island) for turbine/tunnel installation may appear tempting. The construction cost of longer tunnels through a cape need not necessarily be more than that of an artificial dam. As predicted in (3.46), the finite cape width augments the water-level difference by the factor $(1 + b/a)^{3/2}$. However, a preliminary estimate based on the Darcy–Weisbach formula indicates that the friction loss in long turbine tunnels is very great even for modest b/a. Therefore, a thin dam is likely to be the best choice from the engineering point of view. The eventual feasibility of DTP must, of course, await further studies of economic and environmental impacts.

	a (km)	20	30	40	50
	N	1000	1500	2000	2500
	Σ_N	719	1079	1438	1798
$V=1$ (m s^{-1})	$\lvert\Delta\eta_0\rvert$	0.594	0.891	1.188	1.485
	P	0.400	1.100	2.260	3.950
$V=2$ (m s^{-1})	$\lvert\Delta\eta_0\rvert$	1.680	2.520	3.360	4.200
	P	1.132	3.112	6.592	11.170

TABLE 1. Maximum water-level difference $|\Delta\eta_0|$ (m) and total power output P (GW) for various dam lengths a (km) and tidal current speeds $V=1$ and 2 m s^{-1}. The coefficient product C_eC_d is assumed to be 1.0.

6. Summary

The diffraction of tides by a small island and a small cape of elliptical shape is derived by the method of matched asymptotics. To order $O(k^2a^2)$, the scattered wave is represented by the sum of a source and a doublet. By matching only with the linear approximation of the ambient tide, the near field and the doublet strengths are determined. The source strength must, however, be found by matching the near field with the quadratic terms in the inner expansion of the ambient tide. In doing so, the equivalence of the mathematical approach of Martin & Dalrymple (1988) and the physical reasoning of Rayleigh (Strutt 1897) is pointed out. Our results on scattered waves complement the potential-theoretic approximation of the near field by Proudman (1915). As an application to a novel idea of harvesting tidal power, the prospects of a thin dam connected to a straight coast are quantitatively assessed. More accurate prediction requires, of course, computational and physical simulations based on detailed tidal records, the coastal bathymetry and good design of turbines and tunnels.

Acknowledgements

I am grateful to Dr Y. Li for plotting figures 1–3.

Declaration of interests

The author reports no conflict of interest.

Appendix A. Pole strengths for a circular island according to the exact solution

It is convenient to use the formula in Martin (2001)

$$\zeta=\zeta_{inc}+\zeta_{sc}, \tag{A 1}$$

with

$$\zeta_{inc}=\sum_{-\infty}^{\infty}(-\mathrm{i})^n\mathrm{J}_n(kr)\mathrm{e}^{-\mathrm{i}n(\theta-\theta_i)},\quad \zeta_{sc}=\sum_{-\infty}^{\infty}(-\mathrm{i})^n\zeta_n\mathrm{H}_m(kr)\mathrm{e}^{-\mathrm{i}n(\theta-\theta_i)} \tag{A 2a,b}$$

(Martin's θ_i has been changed to $-\theta_i$ and i to $-i$, since his time factor is $\mathrm{e}^{-\mathrm{i}\omega t}$.) And

$$\zeta_n=-\frac{ka\mathrm{J}_n'(ka)-n\beta\mathrm{J}_n(ka)}{ka\mathrm{H}_n'(ka)-n\beta\mathrm{H}_n(ka)}, \tag{A 3}$$

where J and H are Bessel and Hankel functions, respectively. By keeping the first two terms $n=0,1$ and assuming $\theta_i=\pi/2$, one obtains

$$\zeta_{sc}/A=\zeta_0\mathrm{H}_0(kr)-\mathrm{i}\zeta_1\mathrm{H}_1(kr)\mathrm{e}^{-\mathrm{i}(\theta-\pi/2)}+(-\mathrm{i})^{-1}\zeta_{-1}\mathrm{H}_{-1}(kr)\mathrm{e}^{\mathrm{i}(\theta-\pi/2)}. \tag{A 4}$$

For small ka it is easy to show that

$$\zeta_0=-\frac{\mathrm{J}_0'(ka)}{\mathrm{H}_0'(ka)}\approx-\mathrm{i}\frac{\pi}{4}(ka)^2, \tag{A 5}$$

which is formally the same as in a non-rotating sea. Since

$$(-\mathrm{i})\zeta_1\mathrm{H}_1(kr)\mathrm{e}^{-\mathrm{i}(\theta-\pi/2)}=-\left[\frac{ka\mathrm{J}_1'-\beta\mathrm{J}_1}{ka\mathrm{H}_1'-\beta\mathrm{H}_1}\right](\cos\theta-\mathrm{i}\sin\theta)\mathrm{H}_1(kr) \tag{A 6}$$

and

$$(-\mathrm{i})^{-1}\zeta_{-1}\mathrm{H}_{-1}(kr)\mathrm{e}^{\mathrm{i}(\theta-\pi/2)}=\left[\frac{ka\mathrm{J}_1'+\beta\mathrm{J}_1}{ka\mathrm{H}_1'+\beta\mathrm{H}_1}\right](\cos\theta+\mathrm{i}\sin\theta)\mathrm{H}_1(kr), \tag{A 7}$$

where the arguments of all Bessel functions in the brackets are ka, one gets

$$\begin{aligned}\zeta_{sc}=A\mathrm{H}_1(kr)\Bigg\{&-\cos\theta\left[\frac{ka\mathrm{J}_1'-\beta\mathrm{J}_1}{ka\mathrm{H}_1'-\beta\mathrm{H}_1}-\frac{ka\mathrm{J}_1'+\beta\mathrm{J}_1}{ka\mathrm{H}_1'+\beta\mathrm{H}_1}\right]\\&+\mathrm{i}\sin\theta\left[\frac{ka\mathrm{J}_1'-\beta\mathrm{J}_1}{ka\mathrm{H}_1'-\beta\mathrm{H}_1}+\frac{ka\mathrm{J}_1'+\beta\mathrm{J}_1}{ka\mathrm{H}_1'+\beta\mathrm{H}_1}\right]\Bigg\}.\end{aligned} \tag{A 8}$$

By approximating the Bessel functions for small ka, we find

$$C_1=-A\left[\frac{ka\mathrm{J}_1'-\beta\mathrm{J}_1}{ka\mathrm{H}_1'-\beta\mathrm{H}_1}-\frac{ka\mathrm{J}_1'+\beta\mathrm{J}_1}{ka\mathrm{H}_1'+\beta\mathrm{H}_1}\right]\approx\mathrm{i}\pi(ka)^2\frac{\omega f}{\omega^2-f^2}A \tag{A 9}$$

and

$$S_1=-\mathrm{i}A\left[\frac{ka\mathrm{J}_1'-\beta\mathrm{J}_1}{ka\mathrm{H}_1'-\beta\mathrm{H}_1}+\frac{ka\mathrm{J}_1'+\beta\mathrm{J}_1}{ka\mathrm{H}_1'+\beta\mathrm{H}_1}\right]\approx-\frac{\pi(ka)^2}{2}\frac{\omega^2+f^2}{\omega^2-f^2}A, \tag{A 10}$$

in agreement with (3.27).

Appendix B. Derivatives in elliptic coordinates

Using the rules of orthogonal coordinates one has

$$\boldsymbol{r}=x\boldsymbol{i}+y\boldsymbol{j}=\boldsymbol{i}(c\cosh\mu\cos\nu)+\boldsymbol{j}(c\sinh\mu\sin\nu). \tag{B 1}$$

From the rules of orthogonal coordinates (e.g. Hildebrand 1976, equation (141)), the scale factors are

$$\begin{aligned}h_\mu&=\left|\frac{\partial\boldsymbol{r}}{\partial\mu}\right|=c\left[\sinh^2\mu\cos^2\nu+\cosh^2\mu\sin^2\nu\right]^{1/2}=c\left[\cosh^2\mu-\cos^2\nu\right]^{1/2}\\&=h_\nu=\left|\frac{\partial\boldsymbol{r}}{\partial\nu}\right|.\end{aligned} \tag{B 2}$$

Since

$$\nabla\zeta = \frac{1}{h_\mu}\frac{\partial\zeta}{\partial\mu}\boldsymbol{e}_\mu + \frac{1}{h_\nu}\frac{\partial\zeta}{\partial\nu}\boldsymbol{e}_\nu \tag{B 3}$$

and

$$\mathrm{d}s_\mu = \mathrm{d}n = h_\mu\,\mathrm{d}\mu, \quad \mathrm{d}s_\nu = \mathrm{d}s = h_\nu\,\mathrm{d}\nu, \tag{B 4a,b}$$

it follows that

$$\mathrm{d}s\frac{\partial\zeta}{\partial n} = \frac{1}{h_\mu}\frac{\partial\zeta}{\partial\mu}h_\nu\,\mathrm{d}\nu = \frac{\partial\zeta}{\partial\mu}\,\mathrm{d}\nu, \quad \mathrm{d}s\frac{\partial\zeta}{\partial s} = \frac{1}{h_\nu}\frac{\partial\zeta}{\partial\nu}h_\nu\,\mathrm{d}\nu = \frac{\partial\zeta}{\partial\nu}\,\mathrm{d}\nu. \tag{B 5a,b}$$

Thus (3.29) can be written as

$$k^2 h\int_{\partial S}\boldsymbol{u}\cdot\boldsymbol{n}\,\mathrm{d}s = \mathrm{i}\omega\int_{\partial S}\frac{\partial\zeta}{\partial\mu}\,\mathrm{d}\nu + f\int_{\partial S}\frac{\partial\zeta}{\partial\nu}\,\mathrm{d}\nu. \tag{B 6}$$

REFERENCES

ABEL-HAFZ, A. M., ESSAWY, A. H. & MOUBARK, M. A. M. 1997 The diffraction of Kelvin waves due to an island. *J. Comput. Appl. Maths* **84** (1997), 147–160.

AL-HAWAJ, A. G., ESSAWY, A. H. & FALTAS, M. S. 1991 The diffraction of Kelvin wave due to a narrow headland normal to an infinite coastline. *Acta Mechanica* **86**, 53–63.

BAKER, A. C. 2000 *Tidal Power*. IET Energy Series.

BUCHWALD, V. T. 1971 The diffraction of tides by a narrow channel. *J. Fluid Mech.* **46**, 501–511.

BUCHWALD, V. T. & MILES, J. W. 1974 Kelvin wave diffraction by a gap. *J. Austral. Math. Soc.* **17**, 29–34.

CRIGHTON, D. G. & LEPPINGTON, F. G. 1973 Singular perturbation methods in acoustics: diffraction by a plate of finite thickness. *Proc. R. Soc. Lond.* A **335**, 313–339.

CREASE, J. 1956 Long waves on a rotating earth in the presence of a semi-infinite barrier. *J. Fluid Mech.* **1**, 86–96.

DAI, P., ZHANG, J.-S & ZHENG, J.-H 2017 Predictions for dynamic tidal power and asociated local hydrodynamic impact in the Taiwan strait, China. *J. Coast. Res.* **33** (1), 149–157.

DAI, P., ZHANG, J.-S, ZHENG, J.-H, HULSBERGEN, K., VAN BANNING, G., ADEMA, J. & TANG, Z.-X. 2018 Numerical studies of hydrodynamic mechanisms of dynamic tidal power. *Water Sci. Engng* **11** (3), 220–228.

ESSAWY, A. H. 1984 The diffraction of a Kelvin wave due to a narrow island normal to an infinite coastline. *Arch. Mech.* **36** (1), 21–31.

ESSAWY, A. H. 1995 Diffraction of a Kelvin wave by a circular island using a Green's function technique. *Bull. Cal. Math. Soc.* **87**, 501–510.

GRADSHTEYN, I. S. & RIZHIK, I. M. 1980 *Table of Integrals, Series and Products*. Academic.

GUO, S. & MCIVER, P. 2011 Propagation of elastic waves through a lattice of cylindrical cavities. *Proc. R. Soc. Lond.* **467** (2134), 2962–2982.

HILDEBRAND, F. S. 1976 *Advanced Calculus for Applications*. Prentice-Hall.

HOWE, M. S. & MYSAK, L. A. 1973 Scattering of Poincare waves by an irregular coastline. *J. Fluid Mech.* **57**, 111–128.

HULSBERGEN, K., STEIJN, R., HASSAN, R., KLOPMAN, G. & HURDLE, D. 2005 Dynamic Tidal Power (DTP). In *6th European Wave and Tidal Energy Conf. Glasgow UK*, pp. 217–222.

HULSBERGEN, K., DE BOER, STEIJN, R. & VAN BANNING, G. 2008*a* Dynamic tidal power for Korea. In *1st Asian Wave and Tidal Conference Series*, pp. 1–8.

HULSBERGEN, K., STEIJN, R., VAN BANNING, G., KLOPMAN, G. & FRÖLICH, A. 2008*b* Dynamic Tidal Power – A new approach to exploit tides. In *2nd Int. Conf. on Ocean Energy, Brest, France*, pp. 1–10.

KLEINMAN, R. & VAINBERG, B. 1994 Full low-frequency asymptotic expansion for secondorder elliptic equations in two dimensions. *Math. Meth. Appl. Sci.* **17** (12), 989–1004.

KLOPMAN, G. 2003, Hydrodynamic simulation tool of Active Tidal Power Plant. *Report D18.00-01*. Albatros Flow Research, Inc.

KRUTITSKII, P. A. 2001 The oblique derivative problem for the Helmholtz equation and scattering tidal waves. *Proc. R. Soc. Lond.* A **457**, 1735–1755.

LAMB, H. 1932 *Hydrodynamics*, p. 530. Dover.

LEBLOND, P. H. & MYSAK, L. A. 1987 *Waves in the Ocean*. Elsevier.

LIU, Q. & ZHANG, W.-L. 2014 Hydrodynamic study of phase-shift tidal power system with Y-shaped dams. *J. Hydraul Res.* **52** (3), 356–365.

MARTIN, P. A. 2006 *Multiple Scattering*. Cambridge University Press.

MARTIN, P. A. 2001 On the diffraction of Poincaré waves. *Math. Meth. Appl. Sci.* **24**, 13–925.

MARTIN, P. A. & DALRYMPLE, R. A. 1988 Scattering of long waves by cylindrical obstacles and gratings using matched asymptotic expansions. *J. Fluid Mech.* **188**, 465–490.

MEI, C. C. 2012 Note on tidal diffraction by a coastal barrier. *Appl. Ocean Res.* **36**, 22–25.

MILNE-THOMSON, L. M. 1955 *Theoretical Hydrodynamics*. Macmillan.

PINSENT, H. G. 1971 The effect of a depth discontinuity on Kelvin wave diffraction. *J. Fluid Mech.* **45**, 747–758.

PINSENT, H. G. 1972 Kelvin wave attenuation along nearly straight boundaries. *J. Fluid Mech.* **53** (2), 273–286.

PROUDMAN, J. 1915 Diffraction of tidal waves on flat rotating sheet of water. *Proc. Lond. Math. Soc.* **14**, 89–102.

PROUDMAN, J. 1953 *Dynamical Oceanography*. Methuen.

RHINES, P. B. 1969*a* Slow oscillations in an ocean of varying depth. Part 1. Abrupt topography. *J. Fluid Mech.* **37**, 161–189.

RHINES, P. B. 1969*b* Slow oscillations in an ocean of varying depth. Part 2. Islands and seamounts. *J. Fluid Mech.* **37**, 191–205.

STAMNES, J. J. & SPJELKAVIK, B. 1995 New method for computing eigenfunctions (Mathieu functions) for scattering by elliptical cylinders. *Pure Appl. Opt. J. Eur. Opt. Soc. Part A* **4**, 251–262.

STRUTT, J. W. (LORD RAYLEIGH) 1897 On the incidence of aerial and electric waves upon small obstacles in the form of ellipsoids or elliptic cylinders, and on the passage of electric waves through a circular aperture in a conducting screen. *Phil. Mag.* **XLIV**, 2–52.

VARADAN, V. K. & VARADAN, V. V. (Eds) 1968 *Low and High Frequency Asymptotics – Acoustic, Electromagnetic and Elastic Wave Scattering*. North Holland.

ZHOU, J.-T., FALCONER, R. A. & LIN, B.-L. 2014 Refinement to the EFDC model for predicting the hydro-environmental impacts of barrage across the Severn Estuary. *Renew. Energy* **62**, 491–505.